BMJ Open Ophthalmology

Application of generative adversarial networks in the restoration of blurred optical coherence tomography images caused by optical media opacity in eyes

Zhengfang Wang,[1,2] Shuang Zhou,[3] Yeye Zhang,[3] Jianwei Lin,[1] Jinyan Lin,[4] Ming Zhu,[3] Tsz Kin Ng,[1] Weifeng Yang,[3,5] Geng Wang [1]

To cite: Wang Z, Zhou S, Zhang Y, *et al*. Application of generative adversarial networks in the restoration of blurred optical coherence tomography images caused by optical media opacity in eyes. *BMJ Open Ophthalmology* 2025;**10**:e001987. doi:10.1136/bmjophth-2024-001987

► Additional supplemental material is published online only. To view, please visit the journal online (https://doi.org/10.1136/bmjophth-2024-001987).

ZW and SZ contributed equally.

Received 9 October 2024
Accepted 5 May 2025

[1]Joint Shantou International Eye Center of Shantou University and The Chinese University of Hong Kong, Shantou, China
[2]Qingyuan People's Hospital, Qingyuan, China
[3]School of Physics and Optoelectronic Engineering, Hainan University, Haikou, China
[4]Department of Physics, Shantou University, Shantou, China
[5]Center for Theoretical Physics, Hainan University, Haikou, China

Correspondence to
Dr Geng Wang; wg@jsiec.org

ABSTRACT

Purpose To assess the application of generative adversarial networks (GANs) to restore the blurred optical coherence tomography (OCT) images caused by optical media opacity in eyes.

Methods In this cross-sectional study, a spectral-domain OCT (Zeiss Cirrus 5000, Germany) was used to scan the macula of 510 eyes from 272 Chinese subjects. Optical media opacity was simulated with an algorithm for training set (420 normal eyes). Images for three test sets were from the following: 56 normal eyes before and after fitting neutral density filter (NDF), 34 eyes before and after cataract surgeries and 90 eyes processed by algorithm. GANs of pix2pix was trained with training set and restored blurred images in test sets. Structural similarity index (SSIM) and peak signal-to-noise ratio (PSNR) were used to evaluate the performance of GANs.

Results PSNR for test sets before and after image restoration was 18.37±0.44 and 19.94±0.29 for NDF ($p < 0.01$), 16.65±0.99 and 16.91±0.26 for cataract ($p=0.68$) and 18.33±0.55 and 20.83±0.41 for algorithm regenerated graph ($p < 0.01$), respectively. SSIM for test sets before and after image restoration was 0.85±0.02 and 1.00±0.00 for NDF ($p < 0.01$), 0.92±0.07 and 0.97±0.02 for cataract ($p < 0.01$) and 0.86±0.02 and 0.99±0.01 for algorithm regenerated graph ($p < 0.01$), respectively.

Conclusions GANs can be used to restore blurred OCT images caused by optical media opacity in eyes. Future studies are warranted to optimise this technique before the application in clinical practice.

WHAT IS ALREADY KNOWN ON THIS TOPIC

⇒ Optical media opacities, such as cataracts, can severely blur optical coherence tomography (OCT) images, making them difficult to interpret. Traditional image processing methods struggle to restore these images, but generative adversarial networks (GANs) show promise for improving image reconstruction and reducing noise.

WHAT THIS STUDY ADDS

⇒ This study presents an improved GAN architecture called pix2pix, designed to enhance OCT images in patients with optical media opacities. The results show that pix2pix can restore the details and structures of blurred OCT images with good quality.

HOW THIS STUDY MIGHT AFFECT RESEARCH, PRACTICE OR POLICY

⇒ This study provides significant insights for further exploration of GAN applications in rectifying distortions across different medical imaging modalities. In clinical practice, the pix2pix framework can assist ophthalmologists in accurately interpreting OCT images of patients with optical media opacities, thereby improving diagnostic precision and treatment effectiveness.

INTRODUCTION

Optical coherence tomography (OCT) is a widely used technique in clinical practice, particularly in ophthalmology.[1–4] It can use infrared light to scan the retina through the transparent ocular structures of the eyeball. Therefore, it is an important investigation for retina. However, many retinal diseases are associated with older age, like age-related macular degeneration, glaucoma and diabetic macular oedema. Older patients often have other age-related eye diseases, which may reduce the transparency of the ocular structures, like senile cataract. The OCT images in these patients may be impaired due to the opacity of optical media of the eye. Therefore, it is important to develop a method to repair blurred OCT images from these patients.

Traditional image restoration methods mainly include filtering, model-based methods and variational methods. Filtering methods like mean filtering and median filtering can simply remove noise but are prone to blurring details. Model-based methods, such as Wiener filtering, can suppress noise and preserve details, yet they have limited effectiveness in dealing with complex situations. Variational methods like the total variation model can remove noise and maintain edges, but they

may cause the staircase effect.[5–7] Modern image restoration methods are mainly based on machine learning and deep learning. Machine learning methods, such as support vector machines and random forests, can learn the features of images, but they have poor adaptability to complex tasks. Among deep learning methods, convolutional neural networks[8] can learn the hierarchical features of images and handle various types of image degradation problems. Recurrent neural networks[9] and their variants (such as long short-term memory networks[10] and gated recurrent units) can handle sequential information.[11] GANs, as an important branch of modern image restoration methods, have strong generation ability and good adaptability. GANs have been showing potential in image processing. It has been successfully used to synthesise,[12 13] denoise[14–16] and reconstruct[17–19] images. Previous studies have used GAN to denoise[14–16] ophthalmic OCT images. GANs have shown good generative capabilities and are essential for reconstructing the intricate structures of OCT images.[14] However, all the studies used OCT images that were not from real patient with optical media opacity. To the best of our knowledge, no study has used GAN to restore OCT images of the retina from patient with optical media opacity. The purpose of this study is to use GAN to repair blurred retina OCT images caused by optical media opacity. In recent years, many new GAN architectures have been developed, and common ones include pix2pix[15] and CycleGAN.[20] They have achieved good performance in image-to-image translation tasks. Among them, CycleGAN is suitable for training datasets composed of unpaired images, while pix2pix is suitable for training datasets with paired images. Since paired data are used for model training in this research, the type of GANs adopted in this study is pix2pix.

METHODS

The study was designed following the ethical standards of the Declaration of Helsinki and approved by the ethical committee of Joint Shantou International Eye Center (JSIEC) of Shantou University and The Chinese University of Hong Kong (EC20200609(6)-P23) with written informed consent obtained before the study.

Datasets

Subjects

Chinese subjects, including normal subjects without media opacity and patients with cataract who underwent phacoemulsification combined with intraocular lens implantation at the Department of JSIEC of Shantou University and The Chinese University of Hong Kong, were recruited from December 2018 to October 2020. The inclusion criteria for normal subjects were as follows: (1) age between 18 and 45 years; (2) who have normal retina, without any visual symptoms, and no positive history and signs of systemic or eye diseases; (3) all study eyes had best-corrected visual acuity of at least 20/20 (the Snellen chart), refractive error within ±6 D and intraocular pressure less than 21 mm Hg and (4) the signal strength (SS) ≥6 in the imaging process of clear image. The exclusion criteria were as follows: (1) the subjects were unable to cooperate with the investigation during operation and (2) any eye disease that would influence the OCT imaging. All measurements were performed in the same setting using the same OCT mode and were obtained by a trained technician (ZW). This study followed the tenets of the Declaration of Helsinki and was approved by the Ethics Review Board of JSIEC. An informed consent was obtained from every subject before enrolment in the study.

Dataset creation

B-scan swept-source OCT images were obtained with 6×6 mm macular scanning protocol of a spectral-domain-based OCT (Zeiss Cirrus 5000, Germany) using the follow-up mode. SS is an image quality metric automatically generated by the Zeiss Cirrus OCT device, ranging from 0 to 10. Higher SS values correspond to better image quality. For each target region, three scans were performed, and the image with the highest SS value was selected for analysis to ensure optimal image quality. Images with motion artefacts or insufficient quality for clinical judgement were excluded.

Imaging processing in training set

At present, there are two main methods used to establish optical media opacity as follows. The first method is using physical means to block out some light, such as using a neutral density filter (NDF).[21] The second is using a machine algorithm to blur the clear picture. In this study, we first synthesised hazy cataract-like images from clear images (figure 1). We used the synthesised image pairs to train GANs, which was later used to produce generated images (G).

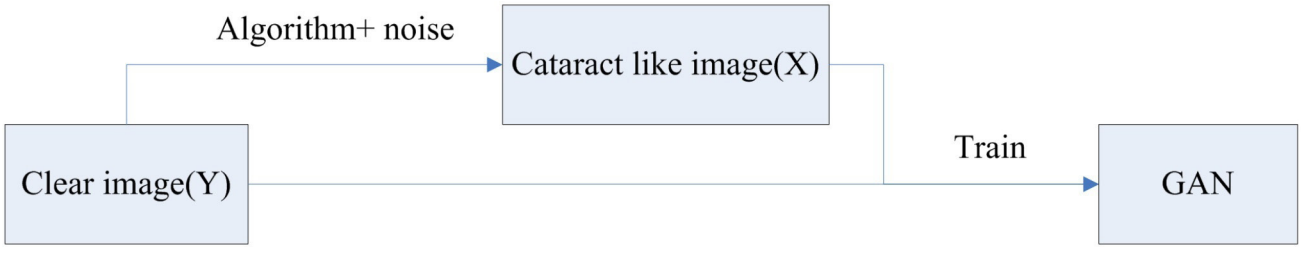

Figure 1 Schematic diagram of the acquiring of cataract-like image. GAN, generative adversarial network.

Table 1 Baseline characteristics of the subjects

Base information	Training set	Test set			P value*
		NDF	Cataract	Generated graph	
Subjects/eyes	210/420	28/56	34/34	62/90	
Age (y), mean±SD	25.2±4.7	25.0±4.2	66.4±9.7	47.7±22.1	< 0.01
Male (%)†	65 (31.0)	8 (28.6)	16 (47.1)	24 (38.7)	0.22
SS, mean±SD	9.0±0.9	8.7±0.9	9.2±0.7	8.9±0.9	0.06
Number of pictures	3702	100	50	770	
PSNR(X/Y), mean±SD	–	18.37±0.44	16.65±0.99	18.33±0.55	< 0.01
SSIM(X/Y), mean±SD	–	0.85±0.02	0.92±0.07	0.86±0.02	< 0.01

*Kruskal–Wallis test.
†χ^2 test.
NDF, neural density filter; PSNR, peak signal-to-noise ratio; SS, signal strength; SSIM, structural similarity index; X, blur image; Y, clear image.

The cataract-like image was obtained by processing the images transformed by Formula 1. Clear image was recorded as 'Y_{train}', and cataract-like image was recorded as 'X_{train}'. After the 'X_{train}' being reconstructed by GANs, it was recorded as a 'G_{train}'.

Formula 1:

$$\text{Image}_{\text{blurred}} = 255 \times \frac{e^{\frac{Image_{clear}}{a}} - 1}{e^{\frac{255}{a}} - 1}$$

where α is a constant set to 70. The value of α represents the degree of clarity or turbidity of the refractive medium, ranging from 0 to 255. In this experiment, the turbidity level of the simulated patient's image is 70, so α is set to 70. Image_{clear} equals the matrix pixel size of a clear image.

There were four datasets in this study (table 1), which included the training set and three test sets as follows: test set of NDF, test set of cataract and test set of algorithm-generated graph. In the training set, all participants (210 Chinese subjects) were normal subjects. There were two types of images in training set: Y_{train} and X_{train}. Y_{train} was acquired directly by OCT, while X_{train} was obtained by processing Y_{train} with the algorithm of formula 1. In the current study, NDF (ZAB, PHTODE, China) was also used to simulate optical media opacity. The transmittance of NDF was 20.2% for a wavelength of 840 nm, with a single pass optical density value (in Log units) of 0.69. In test set NDF, all participants (28 Chinese subjects) were normal subjects. There were two types of images in test set NDF: Y_{filter} and X_{filter}. Y_{filter} was acquired directly by OCT, while X_{filter} was obtained by putting the NDF in front of the normal subjects' eyes (figure 2 (Y_{filter}) and (X_{filter})). In the test set cataract, all participants (34 Chinese subjects) come from patients with cataract, $Y_{cataract}$ and $X_{cataract}$. The images were acquired directly 1-month postoperation and preoperation, respectively (figure 2 ($Y_{cataract}$) and ($X_{cataract}$)). Both the test set cataract and NDF were reprocessed by Photoshop (PS) software. With the centre fovea of image Y as a reference, the centre fovea of image X was dragged to coincide with the reference, rotate and move to make the internal limiting membrane (ILM) of X coincide with the ILM of Y to the greatest extent. Then, the images were trimmed from 1389 × 926 to 1111 × 741 pixels by PS software to remove peripheral mismatched area. If the overlapping area was less than the required range, the image was excluded. Finally, 100 consecutive images were selected for the NDF test set, and 50 consecutive images were chosen for the cataract test set. In the test set generated graph, 28 normal subjects and 34 pseudophakic patients were included. There were two types of images in test set generated graph: $Y_{generated}$ and $X_{generated}$. $Y_{generated}$ is acquired directly by OCT, while $X_{generated}$ is derived through the processing of $Y_{generated}$ by an algorithm (figure 2 ($X_{generated}$) and ($Y_{generated}$)). The GANs model was trained with training set. Three test sets were used to test the GANs model, respectively, after training, as shown in online supplemental figure 1.

Training and test of GANs

Deblur a blurred OCT image based on clear OCT image is an image-to-image translation task. The method used in current study for this translation is pix2pix, which is developed based on GANs.[14 22]

GANs consist of a discriminator network (D) and a generative network (G). GANs are trained by an adversarial learning strategy by means of the adversarial learning between G network and D network. Image-to-image translation is based on an input image to get the desired output image process. The artificial image with high similarity between input image and ground truth can be generated. All images were adjusted to 512×512 pixels from 1389×926 pixels. Data enhancement was performed to increase the amount and type of changes in the training dataset, including horizontal rollover, rotation of 10° and sharpening and adjusting for saturation, brightness, contrast and colour balance in order to expand training set of the GANs model to generate an OCT image with the best anatomical structure. All GANs development and experimentation were done using Python 3.7.6 (Facebook, USA). GANs were trained by the

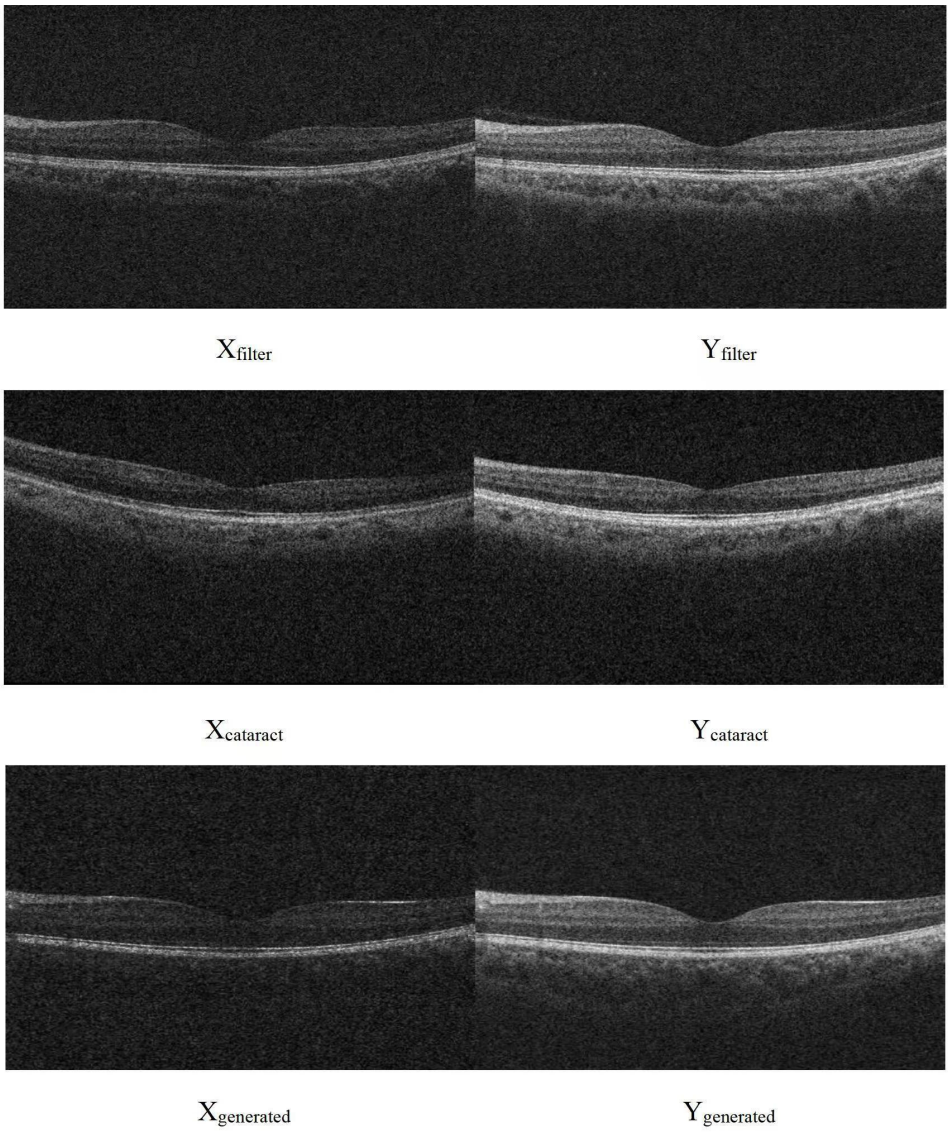

Figure 2 Image comparison of three test sets. X_{filter} is OCT image after adding NDF; Y_{filter} is OCT image before adding NDF; $X_{cataract}$ is OCT image before cataract surgery; $Y_{cataract}$ is OCT image after cataract surgery; $X_{generated}$ is OCT image after processing with formula 1 and $Y_{generated}$ is OCT image before processing with formula 1. NDF, neutral density filter; OCT, optical coherence tomography.

Ubuntu 16.04.4 Long-Term Support Operating System (Canonical Ltd., UK), which features Intel Core i7-2700K 4.6 GHz CPU (Intel, USA), 128 GB RAM and Nvidia GTX 1080Ti 12 GB GPU (Nvidia, USA). Online supplemental figure 1 showed the training and test for the GANs model.

The training parameters used are as follows. The training step size is 1000 steps. During each training session, the discriminative network is optimised once, and the generative network is optimised 19 times. The learning rate is set to 0.0002, and the momentum parameter β in the Adam optimiser is set to 0.5. The core of the method for updating weights during the training of neural networks is the gradient descent method. The gradient descent method adopted in the pix2pix model is the Adam optimisation method. In the minibatch images with an Adam optimiser learning rate of 0.0002, training is carried out through stochastic gradient descent. In this study, it took the GANs approximately 7 hours to complete one round of iteration, and each model was trained for a total of 23 rounds of iteration.

Evaluation metrics and statistical analysis

In order to evaluate the authenticity of synthetic OCT images, all OCT images were evaluated by structural similarity index (SSIM)[23] and peak signal-to-noise ratio (PSNR).[24] PSNR is an objective measure of image quality, often used to evaluate the quality of compressed and reconstructed images. SSIM is a quality measure to measure the similarity between two images. SSIM compares the local information of normalised brightness and the pixel intensity after contrast. Three test sets were used to verify and evaluate the quality and formality of synthetic images. The formulae for calculating the SSIM and PSNR were defined as follows.

Formula 2:

$$SSIM = \frac{(2\mu_x \mu_y + c_1)(2\sigma_{xy} + c_2)}{(\mu_x^2 + \mu_y^2 + c_1)(\sigma_x^2 + \sigma_y^2 + c_2)}$$

where μ_x and μ_y are the mean values of the images, σ_x and σ_y are the SD of the images and σ_{xy} is the covariance of the images. Constants $C_1 = (K_1 L)^2$ and $C_2 = (K_2 L)^2$ are used to avoid zero in the denominator. L is 255 for 8-bit grey images, and K_1=0.01 and K_2 = 0.03 are defined in reference.[25]

Formula 3:

$$PSNR = 10 log_{10}\left(\frac{255^2}{MSE}\right)$$

where MSE is the mean square error.

Python and SPSS software V.22 (IBM-SPSS) was used for statistical analysis, and statistical significance was defined as $p < 0.05$ (two sided). Wilcoxon signed rank test, Kruskal–Wallis test and χ^2 were used to analyse the difference of different types of images.

RESULTS

The mean age was *25.2±4.7* years in the training set, 25.0±4.2 years in the test set NDF, 66.4±9.7 years in the test set cataract and 47.7±22.1 years in the test set *generated graph. There were significant differences in age among groups* ($p < 0.01$, Kruskal–Wallis test). No significant difference was found in gender and SS among groups. The mean PSNR value was *18.37±0.44* in the test set NDF, 16.65±0.99 in the test set cataract and 18.33±0.55 in the test set *generated graph,* respectively ($p < 0.01$, Kruskal–Wallis test). The mean SSIM value was *0.85±0.02* in the test set NDF, 0.92±0.07 in the test set cataract and 0.86±0.02 in the test set *generated graph,* respectively ($p < 0.01$, Kruskal–Wallis test). More baseline characteristics were shown in table 1.

Table 2 shows all the PSNR and SSIM values of all restored images. The PSNR and SSIM values of restored images increased significantly in both test set NDF and test set generated graph ($p < 0.01$, Wilcoxon test). In the test set cataract, the SSIM values of restored images increased significantly ($p < 0.01$, Wilcoxon test).

Table 3 showed the comparison of three test sets. Significant difference among the three test sets was found for both PSNR and SSIM ($p < 0.01$, Kruskal–Wallis test). Online supplemental figure 2 showed the restored images of the test sets.

DISCUSSION

By comparing the PSNR and SSIM values of three test sets, this study showed that the performance of the test set generated graph was the highest, the test set NDF was the second and the test set cataract was the lowest. The result also showed that the quality of the restored image is better than that of the original image, which suggested that GANs can be used to restore the OCT images of patients with media opacity.

In Luo *et al.*' study,[24] based on the dark channel algorithm, a fuzzy fundus image (X) was synthesised from a clear fundus image (Y) using a formula, and CycleGANs were trained to generate a clear fundus image (G) from X using X and Y as inputs. The PSNR was 20.68±3.88, and the SSIM was 0.78±0.08. In this study, the PSNR of the test set generative graph was 20.83±0.41, and SSIM was 0.99±0.01. The PSNR results of this study are lower than those of Luo *et al.*, and the SSIM results are higher than those of Luo *et al.* The possible reasons for the lower PSNR in this study are as follows. First, the cataract–noise programme was used in the process of image processing. Any image processing will affect the fidelity of the image. So, the more complex the image processing, the greater the impact on image quality. Second, the generated image is rather noisy, which may be due to the inconsistency between the feature and distribution of the background noise in the process of obtaining the blurred image and the real image. The possible reasons for the higher SSIM value are as follows. First, the pictures used by Luo *et al.*

Table 2 Comparison of test sets and prerestoration and postrestoration

Evaluation metrics	Test set NDF			Test set cataract			Test set generated graph		
	X/Y	G/Y	P value*	X/Y	G/Y	P value*	X/Y	G/Y	P value*
PSNR	18.37±0.44	19.94±0.29	<0.01	16.65±0.99	16.91±0.26	0.68	18.33±0.55	20.83±0.41	<0.01
SSIM	0.85±0.02	1.00±0.00	<0.01	0.92±0.07	0.97±0.02	<0.01	0.86±0.02	0.99±0.01	<0.01

*Wilcoxon test.
G, restored image; NDF, neural density filter; PSNR, peak signal-to-noise ratio; SSIM, structural similarity index; X, blur image; Y, clear image.

Table 3 Comparative analysis of three test sets

Evaluation metrics	Test set NDF	Test set cataract	Test set generated graph	P value*
PSNR (G/Y)	19.94±0.29	16.91±0.26	20.83±0.41	<0.01
SSIM (G/Y)	1.00±0.00	0.97±0.02	0.99±0.01	<0.01

*Kruskal–Wallis test.
G, restored image; NDF, neural density filter; PSNR, peak signal-to-noise ratio; SSIM, structural similarity index; Y, clear image.

were fundus photos, whereas the pictures used in this study were OCT images of the fundus. SSIM is mainly a measurement of image symmetry. The symmetry of OCT images is better than that of fundus photos.[23] Second, the formula for processing images was different. Although both formulae were based on the previous dark channel algorithm, the formula algorithms were different. Third, the GANs type used by Luo *et al.* is CycleGAN, while the pix2pix was used in this study. CycleGANs are more suitable for training non-paired samples, while pix2pix is more suitable for training paired samples. Based on the principle of GANs-generated confrontation training, pix2pix may have better performance.

The types of pictures in the test set generated graph were the same as those of the training set. As the pictures were similar, the test result was the best. The result of the test set NDF was good. Since the filter mainly causes light attenuation,[21] the light scattering is less and the pictures restoring was easier. The result for the *test set of cataract was the lowest*. Because of the unpredictability of the optical attenuation and scattering, it is difficult to simulate the cataract image completely with the algorithm. Although the image quality has been improved after restoring, it is not enough for clinical application.

In addition, the PSNR value of the test set generated graph was higher than that of the test set NDF and the cataract. This may be due to the fact that the blurred image of the test set generated graph has lost a lot of structural information. For the GANs model, the lesser the image information is, the easier learning the image. So, the performance of the test set generated graph was better. The blurred images of the filter test set and the cataract test set were real images where the effect on light was more complicated and the information was not uniform, especially for cataract image. Since the information was more comprehensive, it was more difficult for model learning in these two models.[26]

In the practical application of OCT blurred image restoration, the type of test set images and processing methods play a critical role in determining the model's performance. This study systematically analysed the applicability and limitations of the pix2pix model in various scenarios by comparing its restoration performance across the generated image test set, the NDF test set and the cataract test set. The results indicated that pix2pix can be used in enhancing image clarity and preserving structural consistency. Current study also identified challenges and areas for improvement when handling complex scenarios.

In the generated image test set, the blurred images lost substantial structural information, simplifying the model's learning process and resulting in the best restoration performance. In contrast, the NDF test set, characterised by minimal light scattering, demonstrated relatively simple restoration while showcasing the model's reliability and stability in processing real-world blurred images. However, the cataract test set posed the greatest challenge due to the randomness and complexity of optical attenuation and scattering, which made it difficult for the algorithm to fully simulate real-world cataract-induced blurring. While the restored images showed noticeable quality improvements, further optimisation is required to meet clinical application standards.

In recent years, GANs have gained widespread attention in the field of OCT blurred image restoration for their exceptional image processing capabilities. This study employed the pix2pix model, based on conditional GANs, and comprehensively evaluated its practical performance through comparisons with traditional methods and experiments conducted on three distinct test sets.

Traditional image restoration methods, including filtering, model-based approaches and variational techniques, offer high computational efficiency but face significant limitations in restoring fine details in complex blurred scenarios.[5–7 27] By contrast, the pix2pix model, leveraging a conditional generation mechanism, excels in handling complex blurring patterns and significantly outperforms traditional methods in both detail restoration and structural consistency.[15 28]

By training on paired blurred and clear images, the pix2pix model establishes a precise mapping relationship. Its key strength lies in its ability to generate highly structurally consistent images while delivering excellent detail recovery. This advantage is particularly evident when addressing OCT blurred images caused by single pathological factors, where pix2pix not only enhances image clarity but also preserves essential pathological features with precision.

The experimental results further validated the pix2pix model's exceptional performance across all three test sets ($p<0.01$). In the generated image test set, the model achieved the best results, with PSNR increasing from 18.33 to 20.83 and SSIM approaching perfection (from 0.86 to 0.99). For the NDF test set, the PSNR rose from 18.37 to 19.94, and the SSIM reached 1.00. In the cataract test set, although the PSNR improvement was modest (from 16.65 to 16.91), the significant increase in SSIM (from 0.92 to 0.97) demonstrated the model's ability to enhance image clarity while effectively preserving pathological features.

There were several limitations in the current study. First, the image resolution in this study was 512×512 pixels. GANs have the potential to produce higher resolution images (eg, 1024×1024 or higher) but require longer training time and bigger training set, which is impractical for this study. Second, other retinal diseases, such as macular hole, epiretinal detachment or pigment epithelium, were not included in the current study. The recovery of OCT image in these diseases requires further optimisation of algorithms. Future work should include restoring images of these retinal diseases and help improve the accuracy of diagnosis for such diseases. Third, the images transformed by our formula were not perfectly the same with cataract patient. In order to get better performance, both the formula for simulating cataract and the GANs

model need further improvement. Since the images of the training set were synthetic and cannot simulate the real cataract completely, future research can incorporate enough pre- and postoperative images into the training set to enhance the applicability in clinical exercise.

CONCLUSIONS

GANs model can be used to restore OCT blurred images caused by optical media opacity in eyes. The restored images have high similarity with original clear images with high image quality. Future studies are warranted to optimise this technique before the application in clinical practice.

Acknowledgements We used the Strengthening the Reporting of Observational Studies in Epidemiology cross-sectional checklist when writing our report.[20]

Contributors Conception and design: GW and WY; Planning and conduct: ZW and SZ; Acquisition of data: YZ and Jinyan Lin; Analysis and interpretation of data: TKN, Jianwei Lin and MZ and GW is the guarantor.

Funding This study was supported by Shantou Science and Technology Project (Grant No.: 190917155269927), 2020 Li Ka Shing Foundation Cross-Disciplinary Research Grant (Grant No.: 2020LKSFG06B).

Competing interests None declared.

Patient and public involvement Patients and/or the public were not involved in the design, or conduct, or reporting, or dissemination plans of this research.

Patient consent for publication Not applicable.

Ethics approval This study involves human participants and was approved by the ethical committee of Joint Shantou International Eye Center of Shantou University and The Chinese University of Hong Kong (EC20200609(6)-P23). Participants gave informed consent to participate in the study before taking part.

Provenance and peer review Part of a topic collection; Not commissioned; externally peer reviewed.

Data availability statement Data are available on reasonable request.

ORCID iD

Geng Wang http://orcid.org/0000-0001-8476-1955

REFERENCES

1 Hee MR, Izatt JA, Swanson EA, *et al*. Optical coherence tomography of the human retina. *Arch Ophthalmol* 1995;113:325–32.
2 Izatt JA, Hee MR, Swanson EA, *et al*. Micrometer-scale resolution imaging of the anterior eye in vivo with optical coherence tomography. *Arch Ophthalmol* 1994;112:1584–9.
3 Swanson EA, Izatt JA, Hee MR, *et al*. In vivo retinal imaging by optical coherence tomography. *Opt Lett* 1993;18:1864–6.
4 Puliafito CA, Hee MR, Lin CP, *et al*. Imaging of Macular Diseases with Optical Coherence Tomography. *Ophthalmology* 1995;102:217–29.
5 Lim JS. *Two-dimensional signal and image processing*. 1989.
6 Gonzalez RC, Woods RE. *Digital image processing*. Prentice Hall, 2002.
7 Rudin LI, Osher S, Fatemi E. Nonlinear total variation based noise removal algorithms. *Physica D: Nonlinear Phenomena* 1992;60:259–68.
8 Krizhevsky A, Sutskever I, Hinton G. ImageNet Classification with Deep Convolutional Neural Networks. 2012.
9 BvM KC, Caglar Gulcehre DB, Fethi Bougares HS, *et al*. Learning phrase representations using rnn encoder–decoder for statistical machine translation. Proceedings of the 2014 Conference on Empirical Methods in Natural Language Processing (EMNLP) EMNLP: Association for Computational Linguistics; 2014:1724.
10 Hochreiter S, Schmidhuber J. Long short-term memory. *Neural Comput* 1997;9:1735–80.
11 Jam J, Kendrick C, Walker K, *et al*. A comprehensive review of past and present image inpainting methods. *Comput Vis Image Underst* 2021;203:103147.
12 Zheng C, Xie X, Zhou K, *et al*. Assessment of Generative Adversarial Networks Model for Synthetic Optical Coherence Tomography Images of Retinal Disorders. *Transl Vis Sci Technol* 2020;9:29.
13 Lazaridis G, Lorenzi M, Ourselin S, *et al*. Improving statistical power of glaucoma clinical trials using an ensemble of cyclical generative adversarial networks. *Med Image Anal* 2021;68:101906.
14 Dong Z, Liu G, Ni G, *et al*. Optical coherence tomography image denoising using a generative adversarial network with speckle modulation. *J Biophotonics* 2020;13:e201960135.
15 Halupka KJ, Antony BJ, Lee MH, *et al*. Retinal optical coherence tomography image enhancement via deep learning. *Biomed Opt Express* 2018;9:6205–21.
16 Kande NA, Dakhane R, Dukkipati A, *et al*. SiameseGAN: A Generative Model for Denoising of Spectral Domain Optical Coherence Tomography Images. *IEEE Trans Med Imaging* 2021;40:180–92.
17 Liu Y, Yang J, Zhou Y, *et al*. Prediction of OCT images of short-term response to anti-VEGF treatment for neovascular age-related macular degeneration using generative adversarial network. *Br J Ophthalmol* 2020;104:1735–40.
18 Yoo TK, Choi JY, Kim HK. Feasibility study to improve deep learning in OCT diagnosis of rare retinal diseases with few-shot classification. *Med Biol Eng Comput* 2021;59:401–15.
19 Tavakkoli A, Kamran SA, Hossain KF, *et al*. A novel deep learning conditional generative adversarial network for producing angiography images from retinal fundus photographs. *Sci Rep* 2020;10:21580.
20 Vitale S, Orlando JI, Iarussi E, *et al*. Improving realism in patient-specific abdominal ultrasound simulation using CycleGANs. *Int J Comput Assist Radiol Surg* 2020;15:183–92.
21 Kok PHB, van Dijk HW, van den Berg TJTP, *et al*. A model for the effect of disturbances in the optical media on the OCT image quality. *Invest Ophthalmol Vis Sci* 2009;50:787–92.
22 Isola P, Zhu J-Y, Zhou T, *et al*. Image-to-image translation with conditional adversarial networks. 2017 IEEE Conference on Computer Vision and Pattern Recognition (CVPR); Honolulu, HI, 2017:1125–34.
23 Wang Z, Bovik AC, Sheikh HR, *et al*. Image quality assessment: from error visibility to structural similarity. *IEEE Trans Image Process* 2004;13:600–12.
24 Luo Y, Chen K, Liu L, *et al*. Dehaze of Cataractous Retinal Images Using an Unpaired Generative Adversarial Network. *IEEE J Biomed Health Inform* 2020;24:3374–83.
25 Fu H, Wang B, Shen J, *et al*. *Evaluation of retinal image quality assessment networks in different color-spaces*.2019:48–56.
26 Gao Y, Song Y, Yin X, *et al*. Deep learning-based digital subtraction angiography image generation. *Int J Comput Assist Radiol Surg* 2019;14:1775–84.
27 Maru M, C. M. Image Restoration Techniques: A Survey. *IJCA* 2017;160:15–9.
28 Fysikopoulos E, Rouchota M, Eleftheriadis V, *et al*. Optical to Planar X-ray Mouse Image Mapping in Preclinical Nuclear Medicine Using Conditional Adversarial Networks. *J Imaging* 2021;7:262.